ELSEVIER

Determining Aerosol Radiative Properties Using the TSI 3563 Integrating Nephelometer

*Theodore L. Anderson**
JOINT INSTITUTE FOR THE STUDY OF THE ATMOSPHERE AND OCEANS, UNIVERSITY OF WASHINGTON, BOX 351640, SEATTLE, WA 98195-1640, USA.

John A. Ogren
NOAA/CLIMATE MONITORING AND DIAGNOSTICS LABORATORY, 325 BROADWAY, BOULDER, CO 80803, USA

ABSTRACT. Methods for reducing and quantifying the uncertainties in aerosol optical properties measured with the TSI 3563 integrating nephelometer are presented. For nearly all applications, the recommended calibration gases are air and CO_2. By routinely characterizing the instrumental response to these gases, a diagnostic record of instrument performance can be created. This record can be used to improve measurement accuracy and quantify uncertainties due to instrumental noise and calibration drift. When measuring scattering by particles, size segregation upstream of the nephelometer at about 1 μm aerodynamic diameter greatly increases the information content of the data for two reasons: one stemming from the independence of coarse and fine particles in the atmosphere, and the second stemming from the size dependence of the nephelometer response. For many applications (e.g., extinction budget studies) it is important to correct nephelometer data for the effects of angular nonidealities. Correction factors appropriate to a broad range of sampling conditions are given herein and are shown to be constrained by the wavelength dependence of light scattering, as measured by the nephelometer. Finally, the nephelometer measurement is nondestructive, such that the sampled aerosol can be further analyzed downstream. Data from two nephelometers operated in series are used to evaluate this procedure. A small loss of super-μm particles (5–10%) is found, while the sub-μm data demonstrates measurement reproducibility within ± 1%. AEROSOL SCIENCE AND TECHNOLOGY 29:57–69 (1998) **© 1998 American Association for Aerosol Research**

INTRODUCTION

In contrast to greenhouse gases, aerosol particles have variable optical properties that must be studied in the field. The variety of chemical and physical forms exhibited by atmospheric aerosols, as well as their short atmospheric lifetime, dictate that survey measurements of their optical properties be conducted across a wide range of locations and timescales. The TSI 3563 nephelometer is well suited to such measurements because of its uniform, commercial production, relative ease of use, and because it simultaneously measures six important parameters

*Corresponding author.

Aerosol Science and Technology 29:57–69 (1998)

Published by Elsevier Science Inc.

0278-6826/98/$19.00
PII S0278-6826(98)00015-4

with high sensitivity and proven accuracy (Anderson et al., 1996). These six parameters are the total scattering coefficient, σ_{sp}^{λ} (m^{-1}), and the hemispheric backscattering coefficient, σ_{bsp}^{λ} (m^{-1}), at three wavelengths, λ (450, 550, and 700 nm).

A pair of recent papers reviewed the history and theory of nephelometer measurements (Heintzenberg and Charlson, 1996) and presented the specific design and performance characteristics of the model 3563 (Anderson et al., 1996). The goal of the present paper is to describe a set of calibration, measurement, and data reduction protocols that will optimize its application to studies of aerosol optical properties.

Deploying nephelometers for this purpose demands accurate calibration and consistent sampling practice to ensure that the six measured parameters are mutually intercomparable and that data collected by one nephelometer at one time and place can be compared to data from other nephelometers at other times and places. The two most important aspects of the sampling system are the particle size selection imposed by the nephelometer inlet and the relative humidity (RH) at which both the size selection and the light scattering measurements take place. The strategy discussed in this paper[1] uses deliberate control of both these variables. Specifically, RH-induced variations are minimized by maintaining a low sample stream RH of 10–40% (achieved by modest heating of 0–10°C), and low-RH size cuts of 10 μm and 1 μm (aerodynamic diameter) are alternately imposed on the sample stream by inertial impaction. Under this strategy, RH-induced variations in light scattering are studied separately by deliberate humidification (Covert et al., 1972; Koloutsou-Vakakis et al., 1994); however, this topic is beyond the scope of the present paper. Here we focus on calibration and size-selection protocols and their consequences for data interpretation.

[1] This sampling strategy has been in use since 1992 at the network of midlatitude aerosol research stations operated by the NOAA Climate Monitoring and Diagnostic Laboratory and has been adopted in the International Global Atmospheric Chemistry series of Aerosol Characterization Experiments.

RECOMMENDED PROTOCOLS

Preferred Calibration Gases

Traditionally, nephelometers have been calibrated using air and CFC-12, thereby spanning a large range of scattering coefficients (from 1 to 15 times σ_{air}). With the restrictions imposed on CFCs by the Montreal Protocol, various substitute high-span gases have been proposed (Horvath and Kaller, 1994) including CO_2, CFC-22, HFC-134a, and SF_6. These are evaluated in Table 1. In terms of calibration accuracy (the overriding consideration for most users), CO_2 is the best choice. This follows from the fact that the model 3563 nephelometer response is known to be extremely linear (Anderson et al., 1996) such that the only issue is to establish the slope of the calibration line with high accuracy. This, in turn, depends on photon-counting statistics during the calibration gas measurement and on how accurately the gas scattering coefficients are known. Equivalent photon-counting statistics can be achieved with any of the high-span gases by adjusting the measurement time. Thus, calibration accuracy reduces to a single issue: how accurately are the gas scattering coefficients known? Because they have been much more extensively studied, the scattering coefficients of air and CO_2 are the most accurately known of the proposed calibration gases. Uncertainties listed in Table 1 are well known for CO_2 but poorly known for the other gases. For example, a major (of order 10%) influence on the scattering coefficient is the depolarization factor (King, 1923), which has been repeatedly measured (and revised—see Young, 1980 and 1981) for air and CO_2 over the last 100 years but remains unknown for all of the alternate high-span gases.

The alternate high-span gases do offer an advantage in terms of required sample time (column 4 of Table 1), which could be important in some experiments (e.g., airborne applications). However, this advantage is

TABLE 1. Evaluation of Alternate Calibration Span Gases

	Cost in May, 1997 ($/kg)	Scattering Ratio with Air[c] σ_{sg}/σ_{air}	Span Gas Measurement Sample Time[i] (min)	Air and Span Gas Measurement[j]	
				Total Time (min)	Cost ($)
CO_2	0.34	2.59 ± 0.9%[d]	30.0	110	0.50
CFC-22[a]	5.3	7.7 ± 2%[e,f]	7.2	87	5.0
HFC-134a[b]	9.2	7.3 ± 3%[e,g]	7.6	88	10.6
SF_6	49.0	6.8 ± 2%[e,h]	8.3	88	38.0

[a] $HCClF_2$. EPA notification required for use.
[b] $H_2C_2F_4$.
[c] Using air scattering coefficients of 27.61, 12.125, and 4.549 (Mm^{-1}) at 273.2°C and 1013.2 mb, uncertain to ± 0.24% as reported by Anderson et al. (1996). The small wavelength dependence of this ratio has been neglected.
[d] CO_2 scattering coefficient determined by air/He calibrated nephelometer and confirmed by independent predictions based on measured refractive index and depolarization factor, as summarized by Anderson et al. (1996). Uncertainty is small and well known.
[e] For span gases other than CO_2, scattering coefficients are based solely on one or two measurements with an air/CO_2 or air/He calibrated nephelometer. The depolarization factors are not known, preventing a theoretical confirmation. Uncertainty is poorly known (i.e., may be larger than indicated here).
[f] Harrison (1977) reports 7.69 ± 0.08. A value of 7.6 ± 0.2 was measured by the author and colleagues at the June 1994 nephelometer workshop (Anderson et al., 1996).
[g] As measured by the author and colleagues at the June 1994 nephelometer workshop (Anderson et al., 1996).
[h] Harrison (1977) reports 6.79 ± 0.07. A value of 6.7 ± 0.2 was measured by the author and colleagues at the June 1994 nephelometer workshop (Anderson et al., 1996).
[i] Sample time only (ignoring time required to flush sample volume and inlet lines) that gives the same photon-counting uncertainty as a 30-minute measurement with CO_2. The effective photon count rate of a span gas is proportional to $\sigma_{sg} - \sigma_{air}$, or to the value for σ_{sg}/σ_{air} above minus one.
[j] Assuming 10-minute air flush, 60-minute air measurement, 10-minute span gas flush, and span gas sample time as listed in previous column, all at a flow of 10 LPM STP. Cost is for span gas only.

largely negated when one takes into account the need to thoroughly flush the instrument and inlet lines prior to commencing the measurement and the need to measure the nephelometer response to air as well as the high-span gas (see column 5 of Table 1).

Finally, while none of the calibration gases is prohibitively expensive, the cost of an equivalently accurate CO_2 measurement is far lower. Moreover, higher costs and further restrictions on the use of F-22, HFC-134a, and SF_6 are possible in the future. It is worth noting that the low cost and ready availability of CO_2 may affect data quality for a practical reason—users need not feel any reluctance to double or triple the flush times, to repeat calibrations, or to make frequent calibration gas measurements as recommended next.

Routine Measurements of Calibration Gases

Because the nephelometer signal (photon-counting rate) is a relative measure of the scattering coefficient, the quality of the aerosol measurements depends fundamentally on how well the instrumental response to the calibration gases is understood. With this in mind, we recommend that frequent measurements of air and CO_2 be used to maintain a diagnostic log of instrument performance. Bracketing aerosol measurements with measurements of air and CO_2 will serve three purposes: (i) to provide immediate and highly precise feedback regarding instrument performance, (ii) to enable correction for calibration drift, thereby improving accuracy, and (iii) to build up a record of instrument noise and drift that can be used to quantify measurement precision. A specific procedure now will be described with results presented in Tables 2 and 3.

The most accurate estimate of particle scattering—call it σ_{best}—takes into account calibration drift. If this quantity has a linear relation to the reported scattering coefficient, σ_m, then,

$$\sigma_{best} = O + S\sigma_m, \quad (1)$$

where O and S are the offset and slope, respectively, of the linear correction scheme. These parameters can be determined from measurements of air and CO_2:

$$S = \frac{\sigma_{k,CO_2} - \sigma_{k,air}}{\sigma_{m,CO_2} - \sigma_{m,air}} \quad (2)$$

$$O = -S\sigma_{m,air}, \quad (3)$$

TABLE 2. Results of Air and CO_2 Measurements over a Two-Month Period

Day of Year (1997)	TOTAL SCATTER			BACKSCATTER		
	450 nm	550 nm	700 nm	450 nm	550 nm	700 nm
Slope, S, of linear correction scheme, Eq. (2)						
70	0.997	0.980	0.969	1.019	0.987	0.978
86	1.018	0.994	0.989	1.036	0.999	1.010
101	1.012	0.978	0.969	1.021	0.988	0.974
120	1.005	0.985	0.986	1.031	0.990	0.995
stdev	0.009	0.007	0.011	0.008	0.005	0.017
Offset, O (Mm^{-1}), of linear correction scheme, Eq. (3)						
70	0.31	0.05	−0.03	0.16	−0.01	0.01
86	0.09	−0.07	−0.05	0.01	−0.06	−0.06
101	0.21	0.08	0.05	0.10	−0.01	0.01
120	0.05	−0.11	−0.07	−0.08	−0.12	−0.15
stdev	0.12	0.09	0.05	0.11	0.05	0.08
Air noise, $\delta\sigma_{noise,air}$ (Mm^{-1}), as defined in Eq. (5) for 60-second averaging						
70	0.39	0.14	0.11	0.27	0.10	0.10
86	0.33	0.15	0.12	0.27	0.10	0.12
101	0.29	0.13	0.12	0.23	0.10	0.15
120	0.42	0.14	0.12	0.26	0.10	0.11
CO_2 noise, $\delta\sigma_{noise,CO_2}$ (Mm^{-1}), as defined in Eq. (5) for 60-second averaging						
70	0.64	0.20	0.18	0.42	0.15	0.13
86	0.61	0.22	0.20	0.36	0.17	0.15
101	0.57	0.23	0.17	0.40	0.13	0.13
120	0.70	0.28	0.17	0.33	0.15	0.11

stdev = standard deviation.

where the subscripts k and m refer to the known scattering coefficient of a given gas and the reported nephelometer measurement, respectively. Recall that the value reported by the nephelometer includes an automatic subtraction of $\sigma_{k,air}$ based on the measured temperature and pressure such that $\sigma_{m,air}$ would equal zero for a perfectly calibrated nephelometer. Both $\sigma_{m,air}$ and σ_{m,CO_2} are assumed to be averages over long (e.g., 30-minute) sample times following a thorough flushing of the instrument and in-

TABLE 3. Results of Filtered Air Measurements on 7 Nephelometers

	TOTAL SCATTER			BACKSCATTER		
	450 nm	550 nm	700 nm	450 nm	550 nm	700 nm
Air noise, $\delta\sigma_{noise,air}$ (Mm^{-1}), as defined in Eq. (5) for 60-second averaging						
ave	0.36	0.19	0.20	0.23	0.11	0.17
stdev	(0.26)	(0.13)	(0.07)	(0.13)	(0.07)	(0.06)
Wall scatter, W (Mm^{-1}), as defined in Eq. (7)						
ave	3.1	3.2	4.6	1.4	1.3	3.1
stdev	(1.0)	(0.7)	(1.3)	(0.7)	(0.5)	(0.8)
Offset variability, δO (Mm^{-1}), derived from repeated re-zeroings over a 12-hour period						
ave	0.14	0.07	0.08	0.10	0.05	0.07
stdev	(0.14)	(0.07)	(0.03)	(0.08)	(0.04)	(0.03)

ave = average; stdev = standard deviation.

let tubing. The values σ_k required by the equations above can be calculated from the data in Table 1 (see column 3 and footnote c) and the measured pressure and temperature, using,

$$\sigma_k(T, P) = \sigma_k(STP)\frac{273.2}{T}\frac{P}{1013.2}. \quad (4)$$

O and S should be determined immediately following each set of air and CO_2 measurements. This provides the user with precise, relevant, and easily understood diagnostic information as displayed in Table 2. Note that S indicates the fractional slope error, and O indicates the offset error (in units of Mm^{-1}) for each of the six measured parameters.

Gas measurements serve an additional purpose of providing an empirical measure of instrument noise[2]:

$$\delta\sigma_{noise} = \text{stdev}[\sigma_{m,gas}(\tau)], \quad (5)$$

where, as indicated, the calculated standard deviation is a function of the averaging time, τ. Measured values of $\delta\sigma_{noise,air}$ for 60-second averaging are given in Tables 2 and 3. A previous work (Anderson et al., 1996) showed that nephelometer noise is well explained by photon-counting uncertainty; that is, that it scales with one over the square root of total photons counted during a given averaging time. This allows noise levels determined with gases to be used to predict noise levels for arbitrary particle scattering coefficients and averaging times:

$$\delta\sigma_{sp,noise}(\sigma_{sp}, \tau) = 2\text{stdev}[\sigma_{m,gas}(\tau_0)]\sqrt{\frac{\tau_0}{\tau}}\sqrt{\frac{\sigma_{sp} + \sigma_{air} + W}{\sigma_{sg} + W}}, \quad (6)$$

where the factor of 2 produces an uncertainty estimate appropriate to 90% confidence, σ_{air} and σ_{sg} are the scattering coefficients of air and the measured gas, respectively, and W is the wall scatter constant determined during the nephelometer calibration. Wall scatter can be calculated from quantities given in the manufacturer's configuration file[3] created after each recalibration:

$$W = B_{ts} - R \quad (7a)$$

$$W_b = B_{bs} - K_4R, \quad (7b)$$

where W and W_b are the wall scatter values for total scatter and backscatter, respectively, B_{ts} and B_{bs} are the listed "Zero Baseline" values for total scatter and backscatter, respectively, R is the listed "Rayleigh Scatter" value (that is, $\sigma_{k,air}$ adjusted for temperature and pressure), and K_4 is the listed calibration factor for backscatter. All these parameters exist for each of the three nephelometer wavelengths. Measured wall scatter values are given in Table 3.

From multiple measurements of the calibration gases over time, the uncertainty in any given measurement of σ_{sp} due to calibration drift, $\delta\sigma_{sp,drift}$, can be calculated as,

$$\delta\sigma_{sp,drift}(\sigma_{sp}) = \sqrt{(2\delta O)^2 + (2\delta S\sigma_{sp})^2}, \quad (8)$$

where δO and δS are the standard deviations of O and S from repeated determinations and the factors of 2 are used, as in Eq. (6), to produce a 90% confidence uncertainty level. This quantity could also be calculated from multiple calibrations over time by replacing O with W (defined in Eqs. 7a and 7b) and S with the manufacturer's calibration constant, K_2.

The quantities in Eqs. (6) and (8) can be combined into an estimate of precision uncertainty:

$$\delta\sigma_{sp,precision}(\sigma_{sp}, \tau) = \sqrt{\delta\sigma^2_{sp,noise} + \delta\sigma^2_{sp,drift}}. \quad (9)$$

The value of this quantity is that it allows nephelometer measurements separated in

[2] Throughout the text, the symbol "δ" before a variable denotes uncertainty in that variable. Thus "$\delta\sigma_{noise}$" denotes uncertainty in the measured scattering coefficient due to noise.

[3] This file is named "nephcnfg.dat" and is overwritten with each new calibration. An additional file named "nephcal-.dat" contains the photon-count rates during the calibration and also is overwritten. Since these files contain vital diagnostic information, another important protocol specific to the current operating software is to save every new version of these files, e.g., by copying them to unique file names.

Aerosol Science and Technology
29:1 July 1998

time or space to be compared. That is, it provides a solid basis for assessing whether or not measured differences in aerosol optical properties are significant. The use of this quantity is illustrated below with data from two nephelometers operated in series.

When measuring calibration gases, noise levels for all six parameters can be kept below 1% by using measurement times of 60 minutes for air and 30 minutes for CO_2. These measurements must be preceded by a thorough flushing of the nephelometer and inlet lines (i.e., several volume exchanges where the nephelometer itself can be treated as a stirred reactor with a volume of 2.5 liters) (Bergin et al., 1997), such that the total procedure takes about two hours. A particle counter mounted downstream of the nephelometer provides an excellent check for leaks or inadequate flushing. Similarly, the built-in RH monitor is a useful check for water vapor contamination (e.g., vapor diffusion from walls and/or filters). Gas measurements should be repeated as often as practical and a log maintained of the derived values of S, O, $\delta\sigma_{noise,air}$, $\delta\sigma_{noise,CO_2}$ as exemplified in Table 2.

Selective Sampling/Exclusion of Coarse Mode Particles

First implemented by White and coworkers (1994), the selective sampling/exclusion of coarse mode particles dramatically increases the information content of nephelometer measurements for two reasons. First, fine and coarse mode particles are generally independent phenomena (Whitby, 1978) with separate sources, sinks, and atmospheric lifetimes. Second, the nephelometer response is very different for coarse and fine mode particles, because a much larger fraction of coarse mode light scattering is concentrated into the near-forward lobe which, due to design limitations, is not sensed by the nephelometer. Field data and Mie calculations are presented below to illustrate the value of this procedure in general and to show the desirability of making the coarse/fine cut at a low-RH aerodynamic diameter of 1 μm.

Angular Correction Factors

When using the nephelometer for extinction budget studies, correction factors should be applied to account for the effects of angular nonidealities (primarily, the truncation of near-forward scattering). Calculated values appropriate to a broad range of sampling conditions are given below. In addition, it will be shown that the wavelength dependence of light scattering, as measured by the nephelometer, can be used to constrain these correction factors and that they are much better constrained when coarse mode particles are excluded from the sample stream.

Aerosol Measurements Downstream of a Nephelometer

The nephelometer measurement is intended to be nondestructive[4], such that the aerosol particles can be analyzed further downstream, including by a second nephelometer. (The build-in blower at the nephelometer outlet can be removed for these applications.) Field tests, discussed below, showed a small loss of super-μm particles (5–10%) at a flow rate of 30 liters per minute, while losses of sub-μm particles appeared to be negligible.

ILLUSTRATIVE RESULTS

Field Measurements at a Coastal Station

Two 3563 nephelometers were operated in series (one immediately downstream of the other) at a coastal station (Cheeka Peak, WA, 48°N, 125°W, 480 m). A cut point at $D_{aero} = 1$ μm was achieved with a multi-jet impactor operating at low RH with a greased substrate to prevent bounce. Sample air alternately passed through or around this impactor, located upstream of the first nephelometer, with a five-minute switching time. The first minute of data following each

[4] Possible losses of particulate matter could occur due to impaction or volatilization, but the plumbing design and the modest sample heating are intended to minimize these losses.

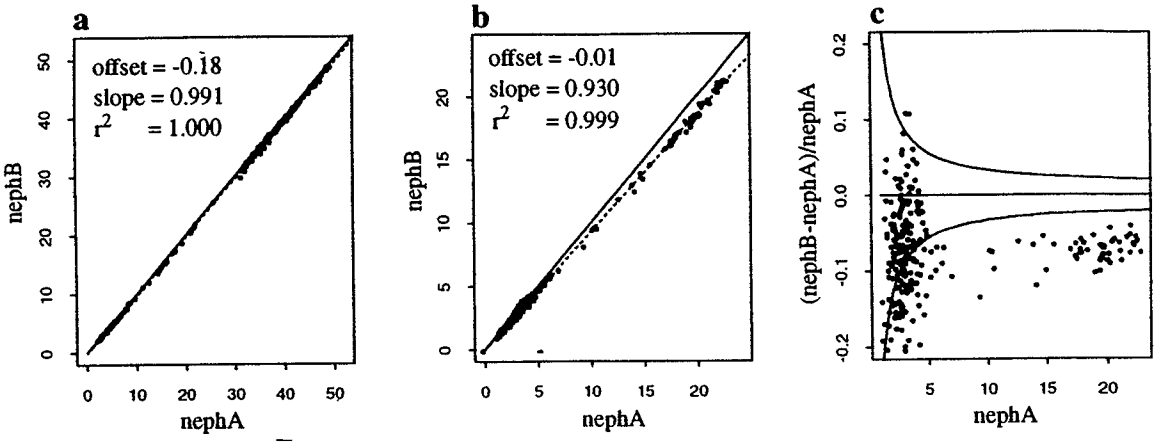

FIGURE 1. Field measurements with two nephelometers in series. 10-minute data collected during nonfoggy conditions over a one-week period. The upstream and downstream units are designated nephA and nephB, respectively. (a) and (b) show nephelometer comparisons of σ_{sp}^{550} for sub- and super-μm particles, respectively (units: Mm^{-1}). (c) shows the relative discrepancy between the two units for super-μm σ_{sp}^{550} as a function of the magnitude of scattering. The solid lines indicate the precision uncertainty calculated from Eq. (9).

switch was discarded. Note that the sub-μm aerosol was measured directly, while scattering by super-μm particles must be determined by subtracting the sub-μm measurements from measurements when the 1 μm impactor was not in line. During one week of sampling in the summer of 1995, a variety of concentrations and air masses were encountered. After discarding fog-impacted samples, just over 40 hours of data remain—241 samples with 10-minute time resolution. Each sample consists of 12 parameters (3 wavelengths, total scatter and backscatter, sub- and super-μm) for both the upstream and downstream nephelometers (denoted "nephA" and "nephB," respectively). Data are reported in units of Mm^{-1} at the nephelometer temperature and pressure (28 $\pm$ 2°C, 950 $\pm$ 10 mb).

Figures 1a and 1b illustrate the discrepancy between the two nephelometers in terms of linear regressions. Correlation coefficients for 9 of the 12 parameters (all but super-μm backscattering, which is noisy due to low signal) are greater than 0.99. For the sub-μm aerosol (e.g., Fig. 1a), regression slopes for all six parameters are within 1% of unity, indicating high precision and little if any loss of particulate matter during transport through nephA. On the other hand, regression slopes for the super-μm aerosol (e.g., Fig. 1b) range from 0.93 to 0.96.

Figure 1c displays the relative discrepancy between nephelometers as a function of concentration (on the x-axis) and in relation to the predicted precision uncertainty arising from noise during both the measurement and the gas calibration. Precision uncertainty was calculated from Eq. (9), using noise and calibration drift data reported previously for these nephelometers (Anderson et al., 1996) and equivalent to that shown in Table 2. Since the discrepancies are well beyond the estimated precision uncertainty, these results provide definitive evidence that a small amount of super-μm particulate matter was lost during transit through the first nephelometer, resulting in a small (5–10%) decrease of super-μm particulate light scattering. To put this loss in context, measured size distributions for the coarse mode aerosol indicated low-RH volume mean diameters of 2–4 μm.

Besides their different plumbing losses, sub- and super-μm particles are revealed by the measurements at our coastal station to be independent atmospheric phenomena with contrasting optical properties. Figure 2 shows data from an entire sampling year (1995). A simple plot of sub-μm versus su-

Aerosol Science and Technology
29:1 July 1998

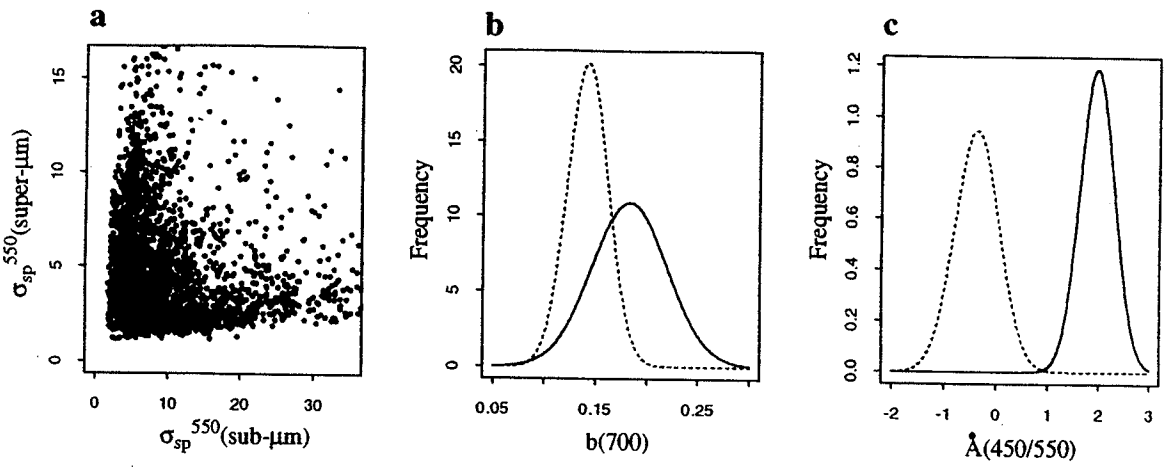

FIGURE 2. Size-segregated nephelometer measurements at a coastal station. Hourly averaged data for nonfoggy conditions during 1995. (a) Relationship between sub- and super-μm particle scattering for σ_{sp}^{550}. (b) Normalized frequency distributions for backscatter ratio at 700 nm. (c) Normalized frequency distributions for measured Ångström exponent over the 450 to 550 nm wavelength range. In (b) and (c), solid and dashed lines correspond to sub- and super-μm particles, respectively.

per-μm scattering (Fig. 2a) reveals the lack of correlation. The optical properties of sub- and super-μm particles are examined in Figs. 2b and 2c in terms of normalized frequency distributions of the backscatter ratio at 700 nm, b(700), and the Ångström exponent over the 450 nm to 550 nm wavelength range, Å(450/550), defined as follows:

$$b(\lambda) = \frac{\sigma_{bsp}^{\lambda}}{\sigma_{sp}^{\lambda}} \tag{10}$$

$$Å(\lambda_1/\lambda_2) = -\frac{\log(\sigma_{sp}^{\lambda_1}/\sigma_{sp}^{\lambda_2})}{\log(\lambda_1/\lambda_2)}. \tag{11}$$

The solid and dashed curves refer to sub-μm and super-μm data, respectively. Differences between the two particle size categories are dramatic. Consequently, to understand the optical properties of the total aerosol it is crucial to understand the fraction of scattering due to each mode. Coarse/fine separation, as recommended herein, provides a convenient means of assessing this fraction and of studying the optical characteristics of each mode.

Theoretical Study of Cut-Size Effects: Calculated Nephelometer Correction Factors

Nephelometer measurements of σ_{sp} and σ_{bsp} contain systematic errors due to angular and wavelength nonidealities. A correction factor, C, may be defined as,

$$C = \frac{\sigma_{true}}{\sigma_{neph}}, \tag{12}$$

where σ_{true} is the Mie-calculated 0–180° or 90–180° scattering coefficient and σ_{neph} derives from a modified Mie-integral (Heintzenberg and Charlson, 1978) using the measured angular sensitivity of the nephelometer. The angular sensitivity of the model 3563 nephelometer is taken from a previous work (Anderson et al., 1996); wavelength nonidealities were shown to be of secondary importance and are neglected here.[5]

To calculate C, it is necessary to take the gas calibration of the nephelometer into account. This is because an implicit effect of the gas calibration is to correct for angular nonidealities as long as nephelometer measurements are made on a Rayleigh-scattering medium (i.e., gases and very small particles). Errors due to angular nonidealities occur only to the extent that the scattering phase function of the measured aerosol dif-

[5] Tables of the measured angular and wavelength sensitivities of the 3563 nephelometer are available from the authors; send requests by email to: tadand@u.washington.edu.

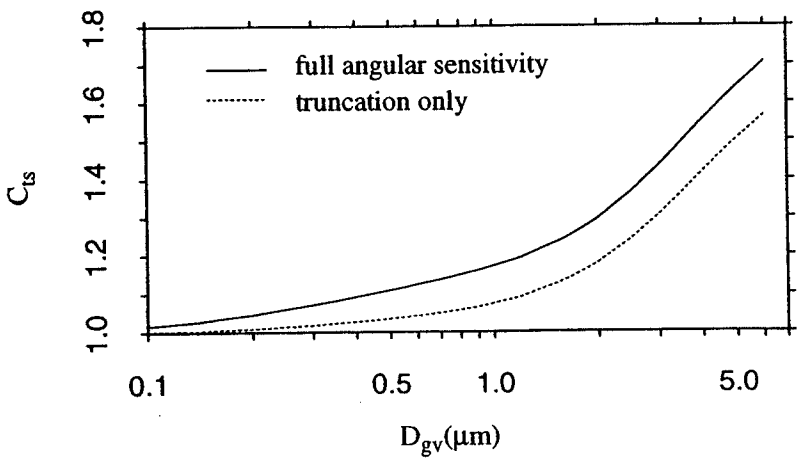

FIGURE 3. Calculated correction factor, C_{ts}, accounting for angular nonidealities in the nephelometer measurement of σ_{sp}^{550}, plotted as a function of the geometric volume mean diameter, D_{gv}, of a lognormal size distribution. Here, the geometric standard deviation was set to 1.8 and a refractive index of 1.46 − 0.00i was used. Angular nonidealities derive from the nonlambertian nature of illumination intensity and from truncation of near-forward-scattered light (from 0 to ~7°), as discussed in the text. The solid line shows the calculated value of C_{ts} when the full angular sensitivity is taken into account, while the dashed line shows C_{ts} calculated when only 0–7° truncation error is considered.

fers from the Rayleigh-scattering phase function. (For a full discussion, see Anderson et al., 1996.)

The total scatter correction, C_{ts}, arises because the nephelometer measurement is biased away from near-forward scattering. The fraction of light scattered in the near-forward direction increases monotonically with particle size for particles diameters below about 5 μm. For this reason, C_{ts} is near unity for very small particles ($D_p < 0.1$ μm) and increases monotonically with particle size (assuming a constant refractive index and a broad enough size distribution to damp out the Mie oscillations), as shown in Fig. 3. Because the wavelength variation of scattering is also sensitive to particle size, it is possible, as will be shown below, to use the measured Ångström exponent (Eq. 11) to constrain C_{ts}. (A similar idea was put forward by Rosen et al., 1997.) Correcting the nephelometer measurement of σ_{sp} for angular nonidealities is required when total extinction due to scattering is of interest—for instance, in extinction budget studies (White, 1990; Malm et al., 1996) or column closure studies (Clarke et al., 1996; Remer et al., 1997).

Two factors contribute to biasing nephelometer sensitivity away from near-forward scattering: truncation error (the geometrical blockage of near-forward-scattered light for angles below about 7°) and nonlambertian error (the slightly noncosine-weighted intensity distribution of illumination light provided by the opal glass diffusor). The dashed curve in Fig. 3 shows what C_{ts} would be if truncation error were the only factor. While truncation error dominates for large particles (where C_{ts} is also large), it is apparent from Fig. 3 that nonlambertian error dominates for sub-μm particles.

In contrast to C_{ts}, the backscatter correction factor, C_{bs}, is always fairly close to unity and is not a monotonic function of particle size. It arises from imperfect separation of light at 90° and unsensed light beyond about 170°. C_{bs} is of interest, for instance, when converting backscatter ratio, $b = \sigma_{bsp}/\sigma_{sp}$, to asymmetry parameter, g, as is required for computing aerosol effects in two-stream radiative transfer models. Formulas available for making this conversion (Marshall et al., 1995) assume "true" values of b. Moreover, knowledge of the uncertainty of C_{bs} and C_{ts} could be propagated usefully into the radiative transfer calculation.

Nephelometer correction factors and their uncertainties, appropriate to a broad range of aerosol populations, are given in Table 4. These were calculated by assuming homogenous spherical particles and bimodal, lognormal size distributions with geometric standard deviations, S_g, of 1.8 and

TABLE 4. Nephelometer Correction Factors for Angular Nonidealities

a) Midpoint ± half range of calculated correction factors for specified conditions[a]

	Total Scatter			Backscatter		
	450 nm	**550 nm**	**700 nm**	**450 nm**	**550 nm**	**700 nm**
No cut	1.29 ± 0.23	1.29 ± 0.23	1.26 ± 0.21	0.981 ± 0.038	0.982 ± 0.038	0.985 ± 0.040
Sub-μm	1.094 ± 0.042	1.073 ± 0.033	1.049 ± 0.023	0.951 ± 0.009	0.947 ± 0.009	0.952 ± 0.010
Super-μm	1.64 ± 0.38	1.51 ± 0.28	1.38 ± 0.20	1.027 ± 0.060	1.026 ± 0.047	1.005 ± 0.051

b) Correction factors for total scatter as a linear function of Ångström exponent using C = a + b*Å[b]

	450 nm				550 nm				700 nm			
			|residual|				|residual|				|residual|
	a	**b**	**mean**	**max**	**a**	**b**	**mean**	**max**	**a**	**b**	**mean**	**max**
No cut	1.365	−.156	0.050	0.22	1.337	−.138	0.046	0.21	1.297	−.113	0.042	0.17
Sub-μm	1.165	−.046	0.010	0.031	1.152	−.044	0.007	0.022	1.120	−.035	0.004	0.014

[a] Bimodal, lognormal size distributions with ranges of volume mean diameters and refractive indices given in text. The range of fine mode mass fraction is 0.9 to 0.1.
[b] Å-values for input to this formula are calculated from Eq. (11) using uncorrected nephelometer measurements of σ_{sp} at two wavelengths; Å(450/550) at 450 nm, Å(450/700) at 550 nm, and Å(550/700) at 700 nm.

geometric volume mean diameters of $0.2 \leq D_{gvF} \leq 0.4$ μm for the fine mode and $2.0 \leq D_{gvC} \leq 4.0$ μm for the coarse mode. Refractive index ranges from $1.40 \leq n \leq 1.52$ for the real part and $0.00 \leq k \leq 0.01$ for the imaginary part were used. These assumptions cover most aerosol populations outside of direct source plumes and when the nephelometer is operated at low relative humidity (RH $\leq$ 50%). For higher RH measurements, larger fine-mode sizes would be appropriate. Similarly, measurements near combustion sources would require higher values of k, and sampling of dust or seasalt near the surface would commonly require larger coarse-mode sizes. Nonspherical shape effects have been neglected in these calculations, which introduces additional, unquantified uncertainty. However, because the angular correction factor arises mostly due to near-forward scattering, which is quite insensitive to shape effects (see, e.g., Mishchenko et al., 1995), we expect this additional uncertainty to be small.

Table 4 and Fig. 4 show the results of these calculations and illustrate several points. First, correction factors for total scatter, C_{ts}, are always greater than unity and are known to sufficient accuracy to justify their use in applications such as extinction budget studies. Second, C_{ts} exhibits a systematic relationship with the measured wavelength dependence of scattering, as represented by the Ångström exponent. This is shown in Figs. 4a and 4b and comes about because both C_{ts} and Å are strong functions of particle size.[6] Using this relationship, C_{ts} is parameterized as a linear function of Å, with the results shown in Table 4b and Figs 4a and 4b. This provides a much more accurate estimate of C_{ts} than adopting a constant value (e.g., the midpoint of the range of possible values, as listed in Table 4a). The latter strategy is appropriate, however, for super-μm particles and for C_{bs} since, in all these cases, there is no useful relationship between C and Å. (See, for instance, Fig. 4c). Finally, the uncertainty data provided in Table 4 demonstrate the utility of segregating sub- and super-μm particles. Such size segregation results in highly accurate information on the sub-μm aerosol—uncertain-

[6] It is interesting to note that the effect of particle refractive index (the real part, n) acts in an orthogonal direction, as shown by the points marked "X" in Fig. 4b. These points represent the highest of the three tested values of n (namely, 1.52).

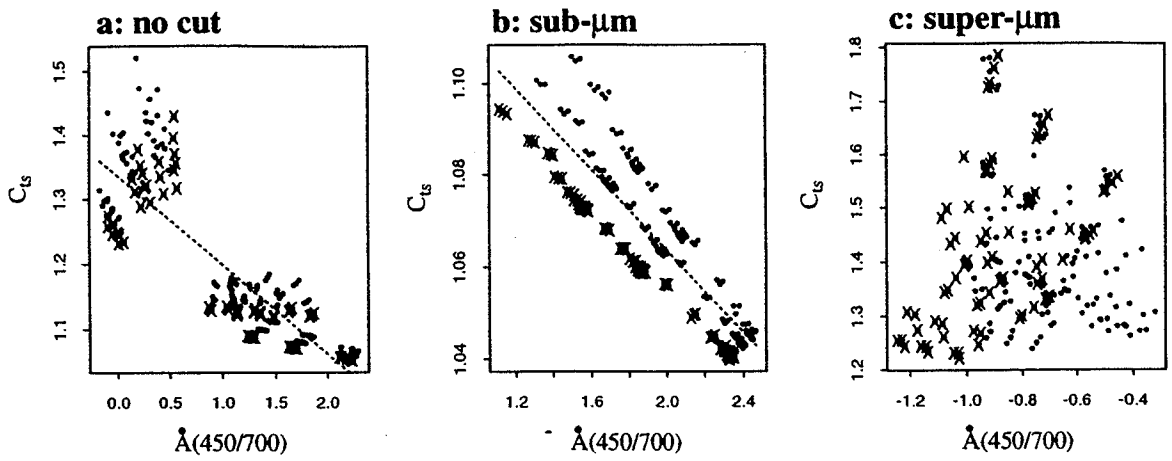

FIGURE 4. Calculated relationship between C_{ts} (as in Fig. 3) and the measured wavelength dependence of light scattering, Å (see Eq. 11). Calculations used a range of bimodal size distributions and refractive indices, as discussed in the text. The fine-mode mass fraction was varied from 10% to 90%. (a) Assuming no size cut, there is a strong relationship between Å and C_{ts}, but the correction factor is large and fairly poorly constrained. (b) Assuming a 1 μm size cut, the relationship is strong and the correction factor is small and well constrained. (c) Assuming an alternating 1 μm size cut, such that derived properties of the super-μm particles can be studied, these super-μm particles are seen to manifest no useful relationship between Å and C_{ts}.

ties are reduced by factors of 5 to 10 with respect to the no-size-cut case, as shown in Table 4b. The reason is obvious from Fig. 4c—the optical properties of super-μm particles result in much larger correction factors that bear no useful relationship to Å. With selective size segregation, optimal nephelometer performance is achieved for sub-μm particles, while useful information on the portion of scattering and backscattering due to super-μm particles is also obtained.

DISCUSSION

Measuring the calibration gases to determine S and O is a convenient means of demonstrating proper instrument performance. Problems stemming from mundane causes such as plumbing leaks, malfunctioning sensors, or software glitches are immediately detectable, making it much less likely that large corrections or loss of data would occur. Extended duration (12–24 hour) measurements of filtered air to determine the quantities listed in Table 3 provide additional performance data for identifying problems that affect noise but not calibration.

Some previous investigators have calculated nephelometer corrections factors by considering truncation error only (e.g., Ensor and Waggoner, 1970) rather than the full angular sensitivity (following Heintzenberg, 1978) which includes the slightly nonlambertian distribution of illumination intensity. As shown in Fig. 3, our calculations indicate that truncation-error-only correction factors will be inaccurate for sub-μm particles, since nonlambertian error dominates in that size range. Depending on particle size, errors of 5–15% could occur. Such errors would be significant if, for example, light absorption were being determined as the difference between total extinction and nephelometer-measured scattering. The calculations shown in Fig. 3 are based on the measured angular sensitivity of the TSI 3563 nephelometer, but the general result probably applies to any nephelometer employing an opal glass diffusor—for instance, the angular sensitivity found by Heintzenberg (1978) was very similar.

Our calculations yield a coarse-mode correction factor of about 1.5 for total scatter at 550 nm, which is considerably lower than the values around 2 derived empirically by

White et al. (1994). This may come about because of the different definitions of coarse mode—low-RH aerodynamic diameter limits are 1.0 and 10 μm herein but were 2.5 and 15 μm in the study by White and coworkers.

While it is important for some purposes to correct nephelometer measurements for angular truncation, in the context of global energy perturbations the nephelometer measurement is a potentially valuable parameter without correction. This is because top-of-atmosphere radiative forcing, like the nephelometer measurement of σ_{sp}, is insensitive to near-forward scattering. Thus, the measured value of σ_{sp} is actually a better proxy for upscatter-to-space than is the "true" value. However, radiative transfer models utilizing this relationship do not presently exist.

CONCLUSIONS

The recommended calibration and measurement protocols can be summarized as follows.

1. The preferred calibration gases for nearly all applications are air and CO_2. As shown in Table 1, these are not only the cheapest, safest, and most convenient to use, but their scattering coefficients are more accurately known than any of the proposed alternate span gases.
2. Optimal accuracy and quantification of uncertainties are facilitated by routine measurements of the calibration gases. Using a simple analysis scheme (Eqs. 1–9), these measurements can be used to maintain a diagnostic record of instrument performance, to improve measurement accuracy, and to quantify instrument noise and calibration drift. Sample results are given in Tables 2 and 3.
3. Coarse mode particles should be periodically excluded from the sample stream. A cut size of 1 μm (aerodynamic diameter at low relative humidity) is recommended. This allows the independent contributions of coarse and fine mode particles to light scattering to be separated, as demonstrated with field data from a coastal station. Further, it fully exploits the potential of the 3563 nephelometer to deliver detailed and highly accurate information on the optical properties of sub-μm aerosol.
4. For extinction budget studies, correction factors for the effects of angular nonidealities should be applied. Values appropriate to a broad range of sampling conditions are given in Table 4, along with uncertainties.
5. Because the nephelometer measurement is essentially nondestructive, aerosol particles can be further analyzed downstream. This technique was evaluated with data from two nephelometers operated in series. A small loss (5–10%) of super-μm particles was observed, and this loss was shown to be beyond the precision uncertainty of the instrument. The sub-μm data showed no evidence of particle losses and demonstrated a measurement reproducibility within $\pm$ 1%.

This research was conducted under the Aerosols component of the NOAA Climate and Global Change Program. It was supported by the National Science Foundation (grant ATM-9320871), by the National Oceanic and Atmospheric Administration (JISAO agreement NAG7RJ0155, contribution no. 446), and by the National Aeronautics and Space Administration (grant NAG 1 1877).

References

Anderson, T. L., Covert, D. S., Marshall, S. F., Laucks, M. L., Charlson, R. J., Waggoner, A. P., Ogren, J. A., Caldow, R., Holm, R., Quant, F., Sem, G., Wiedensohler, A., Ahlquist, N. A., and Bates, T. S. (1996). Performance Characteristics of a High-Sensitivity, Three-Wavelength, Total Scatter/Backscatter Nephelometer, *J. Atmos. Oceanic Technol.* 13: 967–986.

Bergin, M. H., Ogren, J. A., Schwartz, S. E., and McInnes, L. M. (1997). Evaporation of Ammonium Nitrate Aerosol in a Heated Nephelometer: Implications for Field Measurements, *Environ. Sci. Technol.* 31:2878–2883.

Clarke, A. D., Porter, J. N., Valero, F. P. J., and Pilewskie, P. (1996). Vertical Profiles, Aerosol Microphysics, and Optical Closure during the

Atlantic Stratocumulus Transition Experiment: Measured and Modeled Column Optical Properties, *J. Geophys. Res.* 101:4443–4453.

Covert, D. S., Charlson, R. J., and Ahlquist, N. C. (1972). A Study of the Relationship of Chemical Composition and Humidity to light Scattering by Aerosols. *J. Appl. Meteo.* 11:968–976.

Ensor, D. S. and Waggoner, A. P. (1970). Angular Truncation Error in the Integrating Nephelometer, *Atmos. Envir.* 4:481–487.

Harrison, A. W. (1977). Rayleigh Volume Scattering Coefficients for Freon-12, Freon-22, and Sulphur Hexafluoride, *Can. J. Phys.* 55:1898–1901.

Heintzenberg, J. (1978). The Angular Calibration of the Total Scatter/Backscatter Nephelometer, Consequences and Applications, *Staub-Reinhalt. Luft* 38:62–63.

Heintzenberg, J., and Charlson, R. J. (1996). The Integrating Nephelometer: A Review, *J. Atmos. Oceanic Technol.* 13:987–1000.

Horvath, H., and Kaller, W. (1994): Calibration of Integrating Nephelometers in the Post-Halocarbon Era, *Atmos. Environ.* 28:1219–1223.

King, L. V. (1923). On the Complex Anisotropic Molecule in Relation to the Dispersion and Scattering of Light, *Proc. Roy. Soc. London* A104:333–357.

Koloutsou-Vakakis, S., and Rood, M. J. (1994). The (NH4)2SO4-NA2SO4 System: Comparison of Deliquescence Humidities Measured in the Field and Estimated from Laboratory Measurements and Thermodynamic Modeling, *Tellus* 46B:1–15.

Malm, W. C., Molenar, J. V., Eldred, R. A., and Sisler, J. F. (1996). Examining the Relationship among Atmsopheric Aerosols and Light Scattering and Extinction in the Grand Canyon Area, *J. Geophys. Res.* 101:19,251–19,265.

Marshall, S. F., Covert, D. S., and Charlson, R. J. (1995). Relationship between Asymmetry Factor and Backscatter Ratio: Implications for Aerosol Climate Forcing, *Appl. Opt.* 34:6306–6311.

Mishchenko, M. I., Lacis, A. A., Carlson, B. E., and Travis, L. D. (1995). Nonsphericity of Dust-like Tropospheric Aerosols: Implications for Aerosol Remote Sensing and Climate modeling, *Geophys. Res. Lett.* 22:1077–1080.

Remer, L. A., Gassó, S., Hegg, D. A., Kaufman, Y. J., and Holben, B. N. (1997). Urban/Industrial Aerosol: Ground-based Sun/Sky Radiometer and Airborne in Situ Measurements, *J. Geophys. Res.* 102:16849–16859.

Rosen, J. M., Pinnick, R. G., and Garvey, D. M. (1997). Measurement of Extinction-to-Backscatter Ratio for Near-Surface Aerosols, *J. Geophys. Res.* 102:6017–6024.

Whitby, K. T. (1978). The Physical Characteristics of Sulfur Aerosols, *Atmos. Envir.* 12:135–159.

White, W. H. (1990). The Components of Atmospheric Light Extinction: A Survey of Ground-Level Budgets, *Atmos. Envir.* 24a:2673–2679.

White, W. H., Macias, E. S., Nininger, R. C., and Schorran, D. (1994). Size-resolved Measurements of Light Scattering by Ambient Particles in the Southwestern U.S.A., *Atmos. Environ.* 28:909–921.

Young, A. T. (1980). Revised Depolarization Corrections for Atmospheric Extinction, *Appl. Opt.* 19:3427–3428.

Young, A. T. (1981). On the Rayleigh-Scattering Optical Depth of the Atmosphere, *J. Appl. Meteor.* 20:328–330.

Received September 18, 1997; accepted March 12, 1998.